Electronic Supplementary Information (ESI)

Subsurface Passivation and Energy-level alignment of $MAPbI_3$ Film by Constructing Gradient-type 2D/3D Perovskite Structure

Yang Liu[a], Ruixue Lu[a,c], Jiafeng Zhang[a,b], Xin Guo[a]*, Can Li[a]*

[a] *State Key Laboratory of Catalysis, Dalian Institute of Chemical Physics, Chinese Academy of Sciences, Dalian National Laboratory for Clean Energy, 457 Zhongshan Road, Dalian 116023, China.*
[b]*University of Chinese Academy of Sciences, Beijing, 100049, China*
[c] *Department of Chemistry, Fudan University, 2205 Songhu Road, Shanghai 200438, China*

*Prof. Xin Guo: guoxin@dicp.ac.cn; Prof. Can Li: canli@dicp.ac.cn

Experimental Section

Materials and methods

All the chemicals were used as received without further purification, including Methylammonium iodide (MAI), 2-thiophenemethylammonium iodide salt (ThMAI), (99.9%), lead iodide (PbI_2) (99%), 2, 2′,7,7′-13 tetrakis (N, N-di-p-methoxyphenylamine)-9, 9′-Spirobifluorene (Spiro-OMeTAD, 99%), lithium bis(trifluoromethylsulfonyl)-imide (Li-TFSI, 99.95 %,) and 4-tert-butylpyridine (tBP) (96%) all purchased from Xi'an PolymerLight Technology Corp). Dimethylformamide (DMF, 99.8%), dimethylsulfoxide (DMSO, 99.9%), Isopropyl alcohol and chlorobenzene (CB, 99.8%) were all purchased from Sigma Aldrich.

UV-visible spectra of 2D perovskites thin films were measured at room temperature via Cary 5000 UV–Vis–NIR spectrophotometer, Varian Inc, USA. The electrochemical impedance spectra (EIS) were obtained by using an electrochemical workstation (CHI600D) with a frequency range from 1 MHz to 1 Hz, applying a bias of 0.93 V in the dark. The XRD analysis was carried out on Powder X-ray Diffractometer (Rigaku) equipped with cupper X-ray source, (Cu Kα: λ= 1.54 Å) at a voltage of 40 kV and 200 mA currents. The diffraction data were collected with angular range 5-60 degrees (2 theta) with step size

0.02. Scanning electron microscopy (SEM): The SEM images were taken by a Quanta 200F microscope (FEI Company) with an accelerating voltage of 20 kV. Fluorescence spectra were recorded by Shimadzu RF-5301 PC spectrometer and Maya2000Pro optical fiber spectrophotometer.

Device fabrication

Glass/ITO substrates were cleaned with isopropyl alcohol, ethanol, and deionized water in sequence in ultrasonic baths for 30 min and then dried using a nitrogen flow. Then, the substrates were treated with UV-ozone for 20 min. The SnO_2 colloid precursor was obtained from Alfa Aesar (tin(IV) oxide, 15% in H_2O colloidal dispersion). (before use, the particles were diluted by H_2O to 2.67%). The final solution was spin coated onto glass/ITO substrates at 4,000 r.p.m. for 30 s, and then baked on a hot plate in ambient air at 150 °C for 30 min. All ETLs were then UVO-post-treated for 20 min and transferred to the dry air glove box (H_2O < 0.01 ppm) for organic–inorganic halide perovskite deposition below.

The perovskite precursor solution was prepared by dissolving 190.8 mg MAI and 553.2 mg PbI_2 or 580.86 mg PbI_2 in 1 mL of DMF–DMSO solvent mixture at a ratio of 4:2 (v:v) under stirring at 500 rpm overnight. The solution was spin coated onto SnO_2 in a two-step program at 1000 and 5000 rpm for 10 and 20 s in glove box. During the second spin-coating step, 0.1 mL of chlorobenzene was dripped onto the film after 10 s of spin coating at 5000 rpm. The film was transferred to 70 °C hotplate with an initial annealing for 2 minutes, and continuing with another annealing at 120 °C for 10 min. For 2D/3D perovskite film, the ThMAI solution in isopropanol was spin-coated on the top of the 3D perovskite film at 3000 rpm for 30 s and annealed at 100 °C for 5 min. The spiro-OMeTAD solution was prepared with 90 mg spiro-OMeTAD in 1 mL of chlorobenzene added with 36 μL TBP and 22 μL Li-TFSI solution (520 mg Li-TFSI in 1 mL of acetonitrile), then spun at 5000 rpm for 40 s. Finally, a 100 nm gold electrode was thermally evaporated onto the spiro-OMeTAD film and the active area is 0.04 cm^2.

Device characterization

Solar Cell Characterization: The current density verses voltage (*J-V*) curves of the fabricated devices were measured in ambient condition at room temperature by Keithley 2400 source, calibrated with 100 mW cm^{-2} illumination intensity (AM 1.5G). Light intensity-dependent *J−V* curves were obtained by tuning the light source power and calibrating it with the current of the silicon solar cell with a KG5 filter. The external quantum efficiency (EQE) spectrum was obtained using a solar cell spectral response measurement system (Enli technology Co. Ltd). For the hysteresis characterization, the devices were tested from 1.2 to -0.1 V for reverse scan and from -0.1 to 1.2 V for forward scan without any pre-treatment

Environmental stability test: The long-term humidity stability was conducted by storing the unencapsulated devices and thin films inside an environmental chamber at constant humidity and at room temperature. The heat test of unencapsulated devices was carried out inside an environmental chamber at constant temperature and humidity. The light illumination stability test of devices was conducted inside glove box under 1 sun illumination without any encapsulation, using constant light illumination system (Enli technology Co. Ltd).

Mobility measurement: Electron-only devices (ITO/SnO_2/perovskites/PCBM/ Ag were fabricated. Applying Mott-Gurney equations, the dark *J*-V characteristics of the electron-only devices were measured by a Keithley 2400 source.

SCAPS Simulations

Experimentally measured J-V curves were implanted in the software to identify the accuracy of simulation results. Simulation parameters are summarized in Table S6. The voltage of the J-V curve simulation increased from 0 to 1.2 V in 0.02 V steps. SCAPS is an open-source code and can be obtained from https://users.elis.ugent.be/ELISgroups/solar/ projects/scaps upon the conditions requested by the developers Marc Burgelman et al.

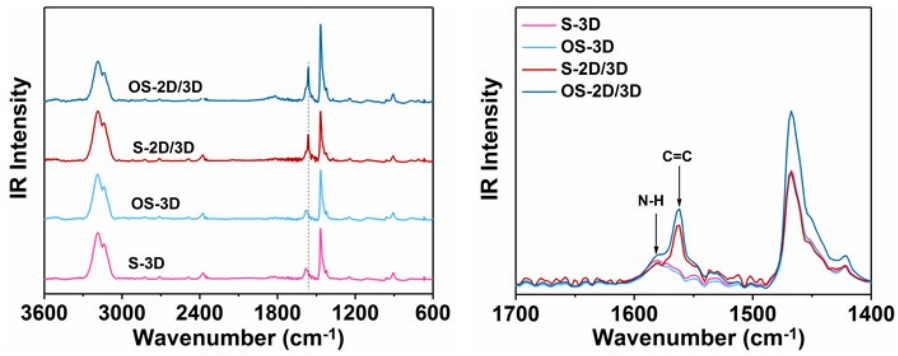

Figure S1. Fourier transform infrared (FTIR) spectra of S-3D, S-2D/3D, OS-3D and OS-2D/3D perovskite films (left), and magnified graph of the peaks between 1700 cm^{-1} and 1400 cm^{-1} (right).

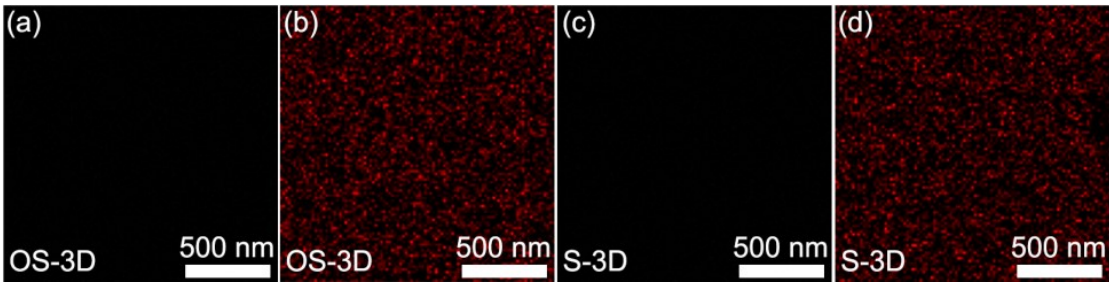

Figure S2. PL imaging of OS-3D and S-3D films by monitoring wavelength at 500-550 nm (a, c), and 740-800 nm (b, d).

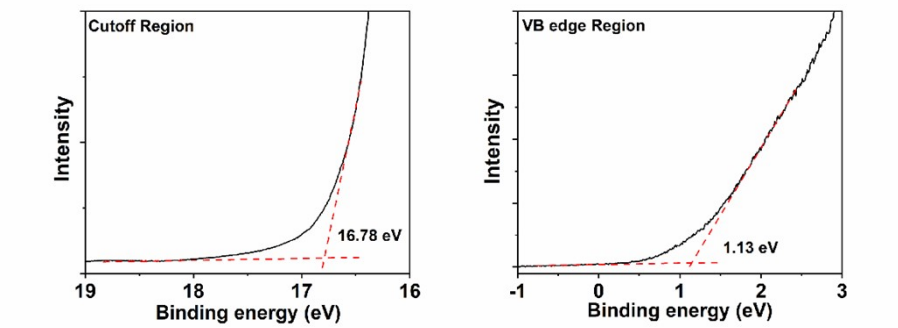

Figure S3. UPS spectra of the cut-off region and valence band edge region of 2D perovskite (ThMA)PbI_4 (n=1) film.

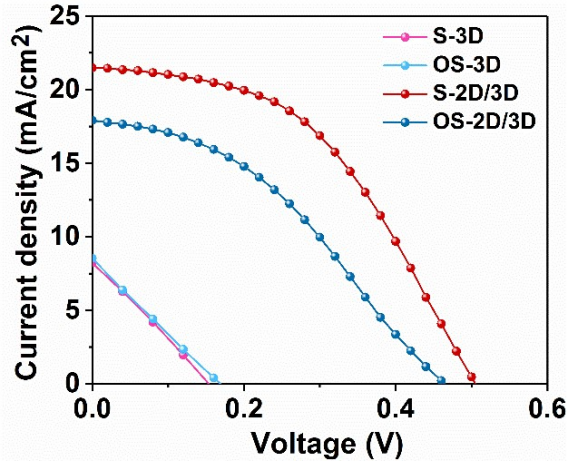

Figure S4. Photocurrent-voltage curves of 3D and 2D/3D PSCs without the organic hole-transporting layer.

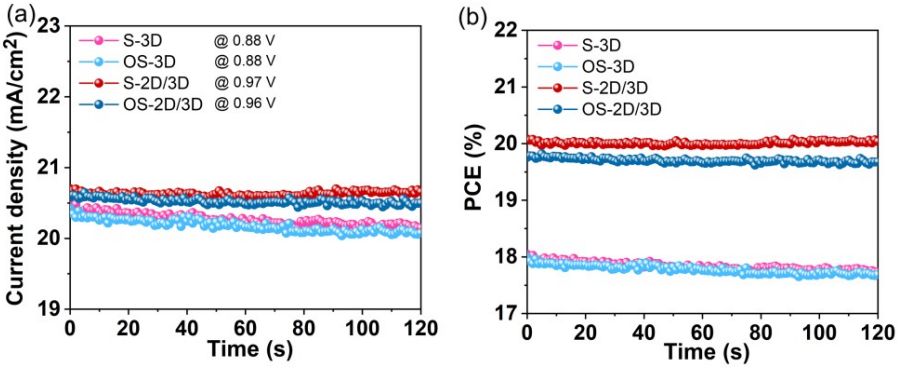

Figure S5. Stabilized photocurrent and PCE measured at a maximum power point of S-3D (0.88 V), S-2D/3D (0.97 V), OS-3D (0.88 V) and OS-2D/3D (0.96 V) PSCs, respectively.

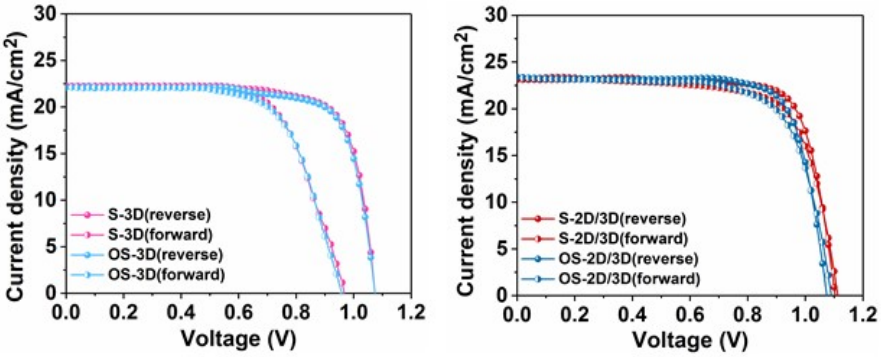

Figure S6. *J–V* curves of 3D and 2D/3D devices with reverse and forward scans.

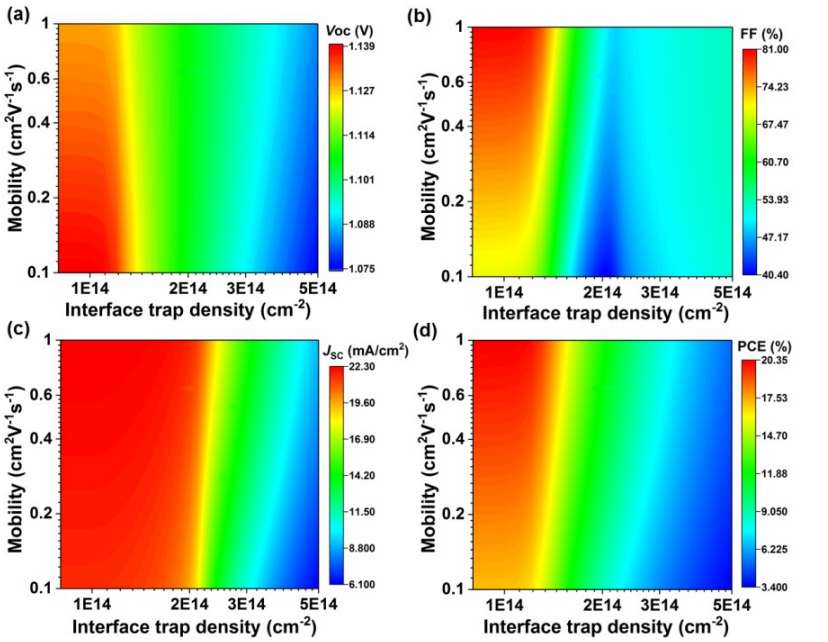

Figure S7. Dependence of the simulated V_{OC}, FF, J_{SC} and PCE on the interface trap density and charge mobility.

Device simulation provides an opportunity to deeply understand the effect of trap density and charge transport on the device performance. We thus evaluated the effect of interfacial trap density of perovskite/HTL and bulk charge mobility on the V_{OC}, FF, J_{SC} and PCE using one-dimensional Solar Cell Capacitance Simulator (SCAPS) calculations, and the basic parameters are listed in the following Table S7. As seen in Figure S5, the interface trap density has a greater effect on the V_{OC}, FF, J_{SC} and PCE. Decreasing the interface trap density can increase V_{OC}, J_{SC} and FF, and hence increasing the PCE. The enhanced charge mobility can increase the FF, but has a slightly negative effect on the V_{OC}, because more charges will be accumulated at the interface and increase the nonradiative charge recombination loss for the same trap density. Thus, the higher V_{OC} of the S-2D/3D PSCs was attributed to the lower trap density, and the better FF of the S-2D/3D PSCs is due to the combination of lower trap density and faster charge transport.

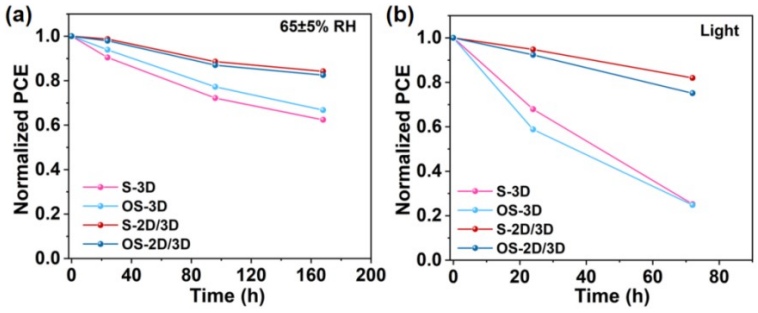

Figure S8. Evolution of the PCE of S-3D, OS-3D, S-2D/3D and OS-2D/3D PSCs under (a) light illumination (AM 1.5G) in glove box and (b) a relative humidity of 65±5% (RH).

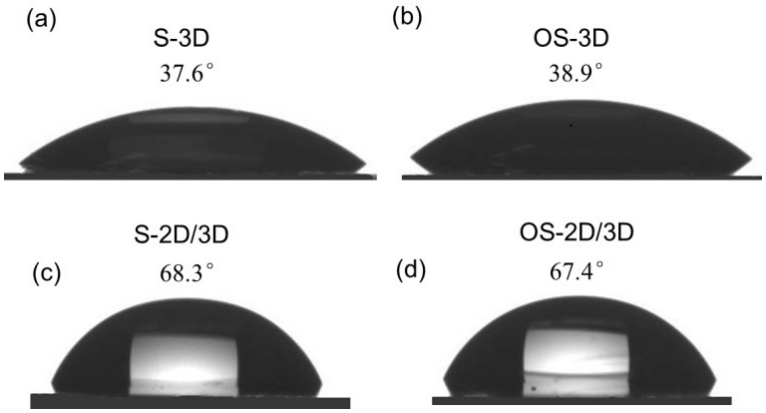

Figure S9. Surface contact angle measurements of water for 3D and 2D/3D perovskite films.

Table S1. Calculated N_t of perovskite films.

Sample	V_{TFL} (V)	N_t (cm^{-3})
S-3D	1.167	8.14×10^{14}
OS-3D	1.161	8.09×10^{14}
S-2D/3D	0.986	6.87×10^{14}
OS-2D/3D	1.003	6.99×10^{14}

Table S2. Fitting parameters of the TrPL spectra of 3D and 2D/3D samples without and with HTL.

Perovskite layer		t_1 (ns)	A_1	t_2 (ns)	A_2	t_{ave} (ns)
Without HTL	S-3D	16.43	167.66	152.69	701.21	149.62
	OS-3D	28.57	93.25	167.93	791.99	164.53
	S-2D/3D	33.35	60.82	314.36	819.35	212.35
	OS-2D/3D	32.58	64.71	191.71	832.22	190.57
With HTL	S-3D	3.21	815.95	34.84	253.27	27.65
	OS-3D	3.37	693.69	29.10	397.82	24.82
	S-2D/3D	2.74	751.63	27.20	280.05	22.03
	OS-2D/3D	2.65	720.02	26.30	358.91	22.95

Table S3. Performance parameters of the devices without HTL.

Device	J_{sc} (mA/cm^2)	V_{oc} (V)	FF (%)	PCE (%)
S-3D	8.52	0.17	24.35	0.35
OS-3D	8.75	0.18	24.02	0.38
S-2D/3D	21.15	0.51	46.62	5.06
OS-2D/3D	17.82	0.47	44.53	3.72

Table S4. Summary of the simulation parameters for 3D and 2D/3D PSCs.

Device	R_s (Ω)	R_{ct} (Ω)	R_{rec} (Ω)
S-3D	35.9	289.1	1310
OS-3D	36.5	282.3	1356
S-2D/3D	35.7	253.7	1622
OS-2D/3D	33.1	260.3	1486

Table S5. The η_{cc} probability of PSCs obtained from J_{ph}-V_{eff} characteristics.

Device	0.1 V	0.2 V	1.2 V
S-3D	58.1 %	87.2 %	99.7 %
OS-3D	58.2 %	87.8 %	99.7 %
S-2D/3D	75.6 %	95.2 %	99.9 %
OS-2D/3D	61.8 %	91.4 %	99.8 %

Table S6. The τ_{IMPS} of PSCs obtained from IMPS measurements.

Device	f_{min} (Hz)	t (μs)
S-3D	56277	2.83
OS-3D	56816	2.80
S-2D/3D	100373	1.59
OS-2D/3D	80242	1.98

Table S7. Basic parameters of PSCs used in SCAPS simulation.

Parameter	ITO	SnO_2	$MAPbI_3$	Spiro-OMeTAD
Thickness (nm)	180	20	500	200
ε_r	2	9	10	3
χ (eV)	3.9	3.9	3.75	2.45
Eg (eV)	3.6	3.2	1.58	3.0
N_c (cm^{-3})	$2*10^{18}$	$2.2*10^{18}$	$2.2*10^{18}$	$2.2*10^{18}$
N_v (cm^{-3})	$1.8*10^{19}$	$1.8*10^{19}$	$1.8*10^{19}$	$2.5*10^{19}$
μ_e ($cm^2\ V^{-1}\ s^{-1}$)	20	20	2	$1.5*10^{-4}$
μ_h ($cm^2\ V^{-1}\ s^{-1}$)	10	10	2	$1.5*10^{-4}$
N_a (cm^{-3})	0	0		$1*10^{20}$
N_d (cm^{-3})	$2*10^{19}$	$2*10^{19}$	$1*10^{19}$	0
N_t (cm^{-3})	$1*10^{15}$	$1*10^{15}$	$2*10^{15}$	$1*10^{15}$